Nonclassical effects in geodesic motion

M. Zhang[*] and Y. Wang[†]

School of Physics, Southwest Jiaotong University, Chengdu 610031, China

Gravity gradient is known as a serious systematic effect in atomic tests of the universality of free fall, where the initial central position and velocity of atoms need to be exactly controlled. In this paper, we study quantum free fall with high-order gravity gradients. It is shown that the cubic terms in the Newtonian potential shall generate a new phase shift in atom interferometers, which depends on the position and velocity uncertainties of the incident atoms. We further investigate the nonclassicality of free fall and show that, due to the cubic potential, the gravitational Wigner equation in phase space of position and velocity is different from the classical Liouville equation. There exists a mass-dependent correction in the dynamical equation regardless of initial state. Nevertheless, this is just a quantum mechanical effect of microparticles, which does not violate equivalence principle that inertia mass is equal to the gravitational mass.

I. INTRODUCTION

By using some modern techniques, such as neutron interferometer [1], atom interferometer (AI) [2–4], and the optical atomic clocks [5–7], gravity near Earth's surface has been measured very precisely. Using AI, the gravitational acceleration was measured in an accuracy of $10^{-9}g$, with $g \approx 9.8$ m/s² [3]. Using optical atomic clocks, the gravitational time dilations due to the height change of less than 1 meter were observed [5]. In addition to interference, the bound state is also a typical nonclassical effect predicted by quantum mechanics. Several experiments [8–10] have demonstrated such phenomena in gravitational potential via the reflecting neutrons above the solid-material surface. Equivalence principle (EP), i.e., inertia mass equals the gravitational mass, is the basis for describing gravitational interaction. There are still no experimental evidences for EP violation [11,12]. However, String theories and some hypothetical experiments of gravity predict EP violation, see, e.g., [13–15]. Recently, scientists propose to test EP with unprecedented accuracy by the program of European Space Agency: the Space-Time Explorer and Quantum Equivalence Space Test mission (STE-QUEST) [16–21]. The advantages of space experiment are the long freely falling time of test particles and the small nongravity noises. Scientists are planning to measure the gravitational acceleration with a high accuracy of $10^{-15}g$ [20,21].

In theory, the calculations for AI's phase shifts are usually based on the uniform gravity and its first-order gradient [22–24], the latter is known as a serious systematic effect in atomic tests of the universality of free fall [25–28].

In this article, we study quantum free fall with high-order gravity gradients. On one hand, the high-order gravity gradients may affect AI's phase shift in the future space laboratory. On the other hand, there has been considerable interest in quantum violation of the universality of free fall [29–33]. Greenberger [29] first introduced this conception by using the gravitational Bohr atoms. The same as Coulomb force, Newtonian gravity is also the central force, so the orbital radius of a particle moving around Earth may be "discrete," which depends on the mass of free fall and therefore contradicts the universality of free fall. However, this still needs a detailed study as the atomic initial state is unlike that of classical particles dropped from some local regimes. In mathematics, it would be very difficult to construct a local initial wave packet in spatial 3-dimensions (wherein the test particles were dropped), via the superposition of "hydrogen atomic eigenstates." Note that, even in classical mechanics, analytically solving the trajectory of free fall as a function of time is not trivial, which refers to the inverse Kepler problem [34].

In this work, we Taylor-expand gravitational potential to be the cubic form. With such nonlinear potential, the positional average of particles couples with its initial position and velocity uncertainties during the process of free falling. Then, there exists a phase shift in AI which depends on the velocity uncertainty of the incident atoms. The phase shift increases with the time of freely falling as t^4, and decreases with Earth's radius as R^2. Thus, this effect is negligible in the ground-based laboratory, because of large R and short t. However, the present systematic effect may be not negligible in the future space experiment due to the gravity of the satellites whose sizes are far smaller than that of Earth, and very long freely falling time of cold atoms.

---
[*]zhangmiao079021@163.com
[†]qubit@home.swjtu.edu.cn

026005-1

We further investigate the nonclassicality of free fall based on the Wigner equation which is known as an effective approach to study the quantum-to-classical transition [35]. With the nonlinear Newtonian potential, the Wigner equation in phase space of position and velocity is different from the classical Liouville equation. There exists a quantum correction in the dynamical equation which depends on the mass of free fall. We propose an approach to solve the multidimensional Wigner equation within the lowest-order quantum correction, and give a numerical estimation on the magnitude of the observable nonclassical effect in real space.

This article is organized as follows. In Sec. II, by using the Newtonian equation (and Heisenberg equation) we calculate the time-dependent position (and positional operator) of a freely falling particle in the gravitational potential of cubic form. The obtained solution of the positional operator takes the same form as that of the classical trajectory in time evolution. In Sec. III., we study the path-dependent phase of AI with the cubic potential, and show that there is a phase shift relating to the initial velocity uncertainty of incident atoms and may be detectable in the space laboratory. We also suggest using the nonuniform magnetic field to simulate gravitational field for demonstrating the predicted effects in the ground-based laboratory. In Sec. IV, we solve the gravitational Wigner equation and discuss the dynamical nonclassicality. Finally, we present our conclusions in Sec. V.

II. POSITION AND POSITIONAL OPERATOR

A. The classical one-dimensional motion

In the region $x, y, z \ll R$ of the displaced Cartesian coordinates $(R + x, y, z)$, we expand the Newtonian potential as

$$
\begin{aligned}
\phi(\mathbf{r}) &= -\frac{GM}{\sqrt{(R + x)^2 + y^2 + z^2}} \\
&\approx gx - \frac{g}{R}x^2 + \frac{g}{2R}(y^2 + z^2) \\
&\quad + \frac{g}{R^2}x^3 - \frac{3g}{2R^2}(y^2 + z^2)x + \cdots,
\end{aligned} \tag{1}
$$

by neglecting the terms of higher order than $(1/R)^2$ and the constant $-GM/R$, where $\mathbf{r} = (x, y, z)$ and $g = GM/R^2$, with gravitational constant $G \approx 6.67 \times 10^{-11}$ N $\cdot$ m$^2 \cdot$ kg^{-2} and the mass M of a spherical gravity source. Following potential (1), the classical motion equation $d^2x/dt^2 = -\partial_x\phi(\mathbf{r})$ along the x-direction reads

$$
\frac{d^2x}{dt^2} \approx -g\left[1 - \frac{2x}{R} + \frac{3x^2}{R^2} - \frac{3(y^2 + z^2)}{2R^2}\right]. \tag{2}
$$

In the ground-based laboratory, the freely falling time of atoms is ultimately limited by the sizes of practical vacuum

installation, for example, the freely falling of 2 seconds needs a height about 20 m. However, the time can be very long in the microgravity system. For example, the biggest gravitational acceleration is $g_s = GM/R_s^2 \approx 6.67 \times 10^{-8}$ m/s^2 at the surface of a sphere of mass $M = 10^3$ kg and radius $R_s = 1$ m. The initial velocity of cold atoms is on the order of $v_0 = 10^{-3}$ m/s, and therefore the characteristic length of motions is $x \sim v_0t_0 + g_st_0^2/2 \approx v_0t_0 = 10^{-2}$ m with the freely falling time $t_0 = 10$ s. As a consequence, the acceleration contributed by the high-order gravity gradients is $3gx^2/R^2 \approx 4 \times 10^{-12}$ m/s^2, with $R = 1.5$ m. This acceleration seems small but may be detectable in the future space experiments with high precision.

Eliminating physical units in the left and right hands of Eq. (2), all quantities in the equation can be temporarily regarded as dimensionless. In terms of small $1/R$, we expand the solution of Eq. (2) as

$$
x(t) = x_0(t) + \frac{1}{R}x_1(t) + \frac{1}{R^2}x_2(t). \tag{3}
$$

Inserting this series back into Eq. (2) results in

$$
\frac{d^2x_0}{dt^2} = -g, \tag{4}
$$

$$
\frac{d^2x_1}{dt^2} = 2gx_0, \tag{5}
$$

$$
\frac{d^2x_2}{dt^2} = 2gx_1 - 3gx_0^2 + \frac{3}{2}g(y^2 + z^2). \tag{6}
$$

The solution of Eq. (4) is well known:

$$
x_0(t) = x_i + v_{xi}t - \frac{1}{2}gt^2, \tag{7}
$$

with x_i and v_{xi} being the initial position and initial velocity along the x-direction. Inserting Eq. (7) into Eq. (5), we have

$$
x_1(t) = gt^2\left(x_i + \frac{1}{3}v_{xi}t - \frac{1}{12}gt^2\right). \tag{8}
$$

For Eq. (6), we must find the solutions of y- and z-directional motions. In those directions, $\partial_y\phi(\mathbf{r}) = 0$ and $\partial_z\phi(\mathbf{r}) = 0$, by neglecting the terms of $1/R$ in potential (1). Therefore, we can use the simplest forms $y(t) = y_i + v_{yi}t$ and $z(t) = z_i + v_{zi}t$ to solve Eq. (6), because $x_2(t)/R^2$ is considered the highest-order correction of nonlinear gravity. Here, (y_i, z_i) and (v_{yi}, v_{zi}) are the initial position and initial velocity in the (y, z) plane. Then the solution of Eq. (6) is given by

$$x_2(t) = \frac{5g^2 t^4}{12} x_i + \frac{11g^2 t^5}{60} v_{xi} - \frac{11g^3 t^6}{360}$$
$$- \frac{3gt^2}{4}(2x_i^2 - y_i^2 - z_i^2) - \frac{gt^4}{8}(2v_{xi}^2 - v_{yi}^2 - v_{zi}^2)$$
$$- \frac{gt^3}{2}(2x_i v_{xi} - y_i v_{yi} - z_i v_{zi}). \tag{9}$$

Finally, the solution of Eq. (3) is shortly written as

$$x(\mathbf{r}_i, \mathbf{v}_i, t) = \alpha x_i + \beta v_{xi} - \gamma$$
$$- \tilde{\alpha}(2x_i^2 - y_i^2 - z_i^2) - \tilde{\beta}(2v_{xi}^2 - v_{yi}^2 - v_{zi}^2)$$
$$- \tilde{\gamma}(2x_i v_{xi} - y_i v_{yi} - z_i v_{zi}), \tag{10}$$

with

$$\alpha = 1 + \frac{gt^2}{R} + \frac{5g^2 t^4}{12R^2}, \tag{11}$$

$$\beta = t\left(1 + \frac{gt^2}{3R} + \frac{11g^2 t^4}{60R^2}\right), \tag{12}$$

$$\gamma = \frac{1}{2}gt^2\left(1 + \frac{gt^2}{6R} + \frac{11g^2 t^4}{180R^2}\right), \tag{13}$$

$$\tilde{\alpha} = \frac{3gt^2}{4R^2}, \qquad \tilde{\beta} = \frac{gt^4}{8R^2}, \qquad \tilde{\gamma} = \frac{gt^3}{2R^2}. \tag{14}$$

The above parameters are rather tedious, but can be verified by numerically solving the exact Newtonian equation (three coupled differential equations):

$$\frac{d^2\mathbf{r}}{dt^2} = \nabla_r \frac{GM}{\sqrt{(R+x)^2 + y^2 + z^2}}, \tag{15}$$

with $\nabla_r = (\partial_x, \partial_y, \partial_z)$, whose solution in the x-direction is denoted by x_{num}. Correspondingly, we temporarily denote the approximate solution (10) as x_{app}, wherein the second-order correction $x_{(2)} = x_{app} - x_0 - (x_1/R) = x_2/R^2$ is the feature in the present work. So, one may compare it with the numerical counterpart $x_{num} - x_0 - (x_1/R)$, based on the given x_0 and x_1 by Eqs. (7) and (8) respectively. Using our estimated parameters in the paragraph below Eq. (2), we found that the analytical solution in short duration is in good agreement with the numerical one, see Fig. 1.

B. Heisenberg equation for positional operator

We now generalize the above perturbation theory into quantum mechanics for computing the time-dependent positional operator of free fall. The quantized Hamiltonian reads $\hat{H} = \hat{\mathbf{p}}^2/(2m) + m\phi(\hat{\mathbf{r}})$, where the momentum operator $\hat{\mathbf{p}} = (\hat{p}_x, \hat{p}_y, \hat{p}_z)$ and position operator $\hat{\mathbf{r}} = (\hat{x}, \hat{y}, \hat{z})$ obey the canonical quantization. According to the Schrödinger equation, the time-dependent state can be
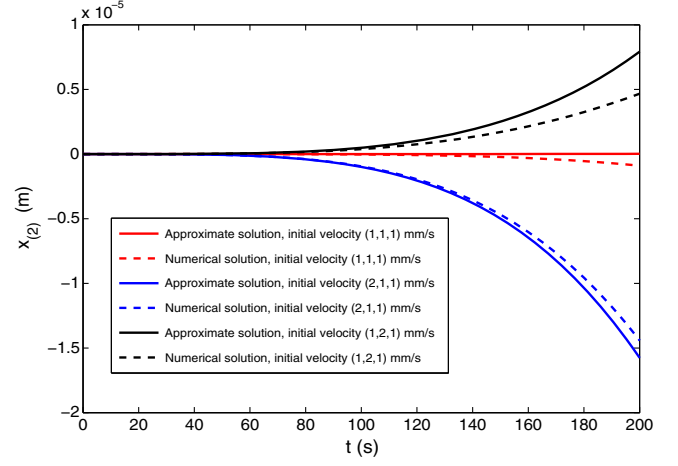

FIG. 1. The solutions of $x_{(2)}$, assuming a free fall was dropped from the initial position $(R + x, y, z) = (1.5 + 0, 0, 0)$ m, near a sphere of mass $M = 10^3$ kg and radius $R_s = 1$ m. The solid lines are obtained from the analytical solution (10) and the dashed lines are the results from the numerical solution of Newtonian Eq. (15). Three initial velocities are considered: $(1, 1, 1)$ mm/s, $(2, 1, 1)$ mm/s, and $(1, 2, 1)$ mm/s.

written as $|\psi\rangle = \exp(-it\hat{H}/\hbar)|i\rangle$ with an initial state $|i\rangle$. Therefore, the time evolution of any observable quantity $\langle i|\hat{O}(t)|i\rangle$ is determined by

$$\hat{O}(t) = e^{\frac{it\hat{H}}{\hbar}} \hat{O} e^{\frac{-it\hat{H}}{\hbar}}. \tag{16}$$

The Heisenberg equation of $\hat{O}(t)$ is

$$\frac{d\hat{O}(t)}{dt} = \frac{i}{\hbar} e^{\frac{it\hat{H}}{\hbar}} [\hat{H}, \hat{O}] e^{\frac{-it\hat{H}}{\hbar}} = \frac{i}{\hbar}[\hat{H}, \hat{O}](t). \tag{17}$$

According to canonical quantization $[\hat{x}, \hat{p}_x] = i\hbar$, we have $[\hat{p}_x^2, \hat{x}] = -i2\hbar\hat{p}_x$ and $[\phi(\hat{\mathbf{r}}), \hat{p}_x] = i\hbar\partial_{\hat{x}}\phi(\hat{\mathbf{r}})$ along the x-direction, and consequently the quantized canonical equations: $d\hat{x}(t)/dt = \hat{p}_x(t)/m$, $d\hat{p}_x(t)/dt = -m[\partial_{\hat{x}}\phi(\hat{\mathbf{r}})](t)$, and $d^2\hat{x}(t)/dt^2 = -[\partial_{\hat{x}}\phi(\hat{\mathbf{r}})](t)$. These equations can be easily generalized into three spatial dimensions, $d\hat{\mathbf{r}}(t)/dt = \hat{\mathbf{p}}(t)/m$, $d\hat{\mathbf{p}}(t)/dt = -m[\nabla_{\hat{r}}\phi(\hat{\mathbf{r}})](t)$, and $d^2\hat{\mathbf{r}}(t)/dt^2 = -[\nabla_{\hat{r}}\phi(\hat{\mathbf{r}})](t)$, with $\nabla_{\hat{r}} = (\partial_{\hat{x}}, \partial_{\hat{y}}, \partial_{\hat{z}})$. Consequently, using the approximate potential (1), the Heisenberg equation of $\hat{x}(t)$ reads

$$\frac{d^2\hat{x}(t)}{dt^2} \approx -g + \frac{2g\hat{x}(t)}{R} - \frac{3g[\hat{x}(t)]^2}{R^2} + \frac{3g[\hat{y}(t)]^2 + 3g[\hat{z}(t)]^2}{2R^2}, \tag{18}$$

which takes the same form to the classical Eq. (2). Thus, the previous approach for solving Eq. (2) is also effective for the present equation.

We also expand the Heisenberg operator as

$$\hat{x}(t) = \hat{x}_0(t) + \frac{1}{R}\hat{x}_1(t) + \frac{1}{R^2}\hat{x}_2(t). \tag{19}$$

Inserting this series into Eq. (18), and using the approximate solutions $\hat{y}(t) = \hat{y} + \hat{v}_y t$, $\hat{z}(t) = \hat{z} + \hat{v}_z t$ in the y- and z-directions, we find

$$\hat{x}_0(t) = \hat{x} + \hat{v}_x t - \frac{1}{2} g t^2, \tag{20}$$

$$\hat{x}_1(t) = g t^2 \left(\hat{x} + \frac{1}{3} \hat{v}_x t - \frac{1}{12} g t^2 \right), \tag{21}$$

and

$$\hat{x}_2(t) = \frac{5 g^2 t^4}{12} \hat{x} + \frac{11 g^2 t^5}{60} \hat{v}_x - \frac{11 g^3 t^6}{360}$$
$$- \frac{3 g t^2}{4} (2\hat{x}^2 - \hat{y}^2 - \hat{z}^2) - \frac{g t^4}{8} (2\hat{v}_x^2 - \hat{v}_y^2 - \hat{v}_z^2)$$
$$- \frac{g t^3}{2} (\hat{x}\hat{v}_x + \hat{v}_x\hat{x}) + \frac{g t^3}{4} (\hat{y}\hat{v}_y + \hat{v}_y\hat{y} + \hat{z}\hat{v}_z + \hat{v}_z\hat{z}), \tag{22}$$

where $\hat{\mathbf{v}} = \hat{\mathbf{p}}/m = (\hat{p}_x, \hat{p}_y, \hat{p}_z)/m$ is the velocity operator. Such a definition is nothing but shows very obvious correspondence between classical and quantum mechanics. Indeed, if one replaces $\hat{\mathbf{r}} = (\hat{x}, \hat{y}, \hat{z})$ and $\hat{\mathbf{v}} = (\hat{v}_x, \hat{v}_y, \hat{v}_z)$ by the classical initial position $\mathbf{r}_i = (x_i, y_i, z_i)$ and initial velocity $\mathbf{v}_i = (v_{xi}, v_{yi}, v_{zi})$ respectively, Eqs. (20)–(22) will exactly reduce to the classical solutions (7)–(9). Inversely, one can directly quantize the classical solutions by $\mathbf{r}_i \to \hat{\mathbf{r}}$ and $\mathbf{v}_i \to \hat{\mathbf{v}}$. In such a way, the product between position and velocity in classical formulas should be rewritten as $\mathbf{r}_i \cdot \mathbf{v}_i = (\mathbf{r}_i \cdot \mathbf{v}_i + \mathbf{v}_i \cdot \mathbf{r}_i)/2$.

There are two purposes for listing out Eqs. (19)–(22). First, they are needed in Sec. III for computing AI's phase in the orders of $(1/R)^0$, $(1/R)^1$ and $(1/R)^2$. Second, they show very obvious correspondence between classical and quantum mechanics. Following these equations, the positional average is given as

$$\langle i|\hat{x}(t)|i\rangle = \alpha \langle i|\hat{x}|i\rangle + \beta \langle i|\hat{v}_x|i\rangle - \gamma$$
$$- \tilde{\alpha}\langle i|(2\hat{x}^2 - \hat{y}^2 - \hat{z}^2)|i\rangle - \tilde{\beta}\langle i|(2\hat{v}_x^2 - \hat{v}_y^2 - \hat{v}_z^2)|i\rangle$$
$$- \tilde{\gamma}\langle i|(\hat{v}_x\hat{x} + \hat{x}\hat{v}_x)|i\rangle$$
$$+ \frac{\tilde{\gamma}}{2} \langle i|(\hat{y}\hat{v}_y + \hat{v}_y\hat{y} + \hat{z}\hat{v}_z + \hat{v}_z\hat{z})|i\rangle. \tag{23}$$

It depends on initial uncertainties of position and velocity, and the position-velocity correlation of the prepared particles ensemble. In any case, compared to the classical statistics based on solution (10), the time-dependent parameters α, β, etc. are not changed. Thus, if the initial state is given by a classical interpretation, for example the Gaussian distribution in Wigner representation [36], then the above time-dependent expectation value is also

classical. In Sec. IV, we will continue to discuss this issue based on the Wigner equation.

III. ATOM INTERFEROMETER

In experiments, the gravitational acceleration of atom is usually measured by AI. In such a device, the atom is manipulated by laser pulses and moves simultaneously along two separate paths to arrive at the detector. In the uniform gravitational field, the path-dependent interferometric phase is independent on the initial position, initial velocity, and the mass of atom. This allows scientists to test EP with very high precision based on the Hamiltonian $\hat{H}_0 = \hat{\mathbf{p}}^2/(2m) + mg\hat{x}$, where the inertia mass is equal to the gravitational mass, $m_I = m_G = m$. However, the interferometric phase will become very complicated when the nonlinear gravity is present. In principle, the atomic initial motions cannot be completely eliminated. Usually, the mathematical derivations for AI's interferometric phase are based on the Feynman path integral [37–39]. In this work, we derive the interferometric phase by using the well-known Zassenhaus formula:

$$e^{\hat{A}+\hat{B}} = e^{\hat{A}} e^{\hat{B}} e^{-\frac{1}{2}[\hat{A},\hat{B}]} e^{\frac{1}{6}[\hat{A},[\hat{A},\hat{B}]]+\frac{1}{3}[\hat{B},[\hat{A},\hat{B}]]} \cdots . \tag{24}$$

It includes an infinite nested commutator of operators $\hat{A}$ and $\hat{B}$, but can be exactly (or approximately) solved within some special cases, for example, $[\hat{A}, [\hat{A}, \hat{B}]]$ and $[\hat{B}, [\hat{A}, \hat{B}]]$ equal to the c-numbers. In the following, we also frequently use the Baker-Campbell-Hausdorff (BCH) formula [40,41],

$$e^{\hat{A}}\hat{B}e^{-\hat{A}} = \hat{B} + [\hat{A}, \hat{B}] + \frac{1}{2!}[\hat{A}, [\hat{A}, \hat{B}]] + \frac{1}{3!}[\hat{A}, [\hat{A}, [\hat{A}, \hat{B}]]] + \cdots . \tag{25}$$

A. Zassenhaus approach for atom interferometer

In a typical AI, see Fig. 2, three laser pulses are applied to probabilistically change atomic momentum by $\hbar\vec{k}$, with $\vec{k}$ being the wave vector of the applied laser pulses. For simplicity, we assume that the y- and z-directional components of $\vec{k}$ are negligible. In Fig. 2, the atom moving along the "up"-path undergos four changes: (a) momentum instantaneously increasing due to the laser scattering at time t_i, (b) freely falling with a duration of $t = t_j - t_i$, (c) momentum suddenly decreasing by the second laser pulse at t_j, and (d) the freely falling in stage $t = t_f - t_j$. So, the state evolution of the up-atom is written as

$$|\uparrow\rangle = \hat{U}(t) e^{-ik\hat{x}} \hat{U}(t) e^{ik\hat{x}} |i\rangle. \tag{26}$$

The operator $\exp(\pm ik\hat{x})$ describes the momentum changes due to the laser scattering, and $\hat{U}(t) = \exp(-it\hat{H}/\hbar)$ is the evolution operator of free fall. There also exists a probability that the atom moves along the "down"-path, i.e., the
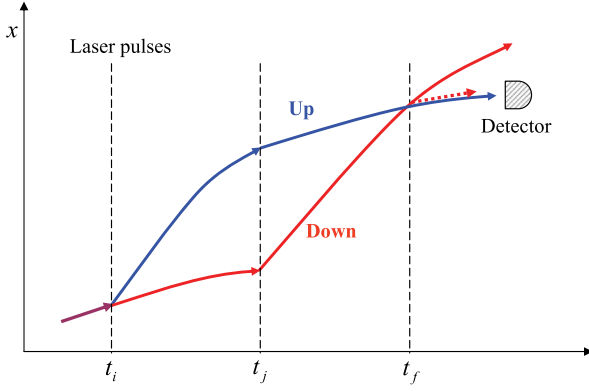
FIG. 2. Sketch for atom interferometer. Three short laser pulses are applied to split and recombine the paths of the traveling atom. The durations for freely falling in each stage are equal, i.e., $t_j - t_i = t_f - t_j = t$. Due to the second-order gravity gradient, the interferometric phase can be shifted by changing the initial momentum uncertainty of the incident atom.

laser induced momentum increasing and decreasing occur at the times t_j and t_f, respectively. Thus, we write the state evolution for the down-path atom as

$$|\downarrow\rangle = e^{-ik\hat{x}}\hat{U}(t)e^{ik\hat{x}}\hat{U}(t)|i\rangle. \qquad (27)$$

The $|\uparrow\rangle$-atom and $|\downarrow\rangle$-atom move both toward to the detector, resulting in an interferometric signal of $\langle\downarrow|\uparrow\rangle$ + c.c., where

$$\langle\downarrow|\uparrow\rangle = \langle i|\hat{U}^\dagger(t)e^{-ik\hat{x}}\hat{U}^\dagger(t)e^{ik\hat{x}}\hat{U}(t)e^{-ik\hat{x}}\hat{U}(t)e^{ik\hat{x}}|i\rangle. \qquad (28)$$

Using the relation $\hat{U}(t)\hat{U}^\dagger(t) = \hat{U}^\dagger(t)\hat{U}(t) = 1$ and the solution $\hat{U}^\dagger(t)\hat{x}\,\hat{U}(t) = \hat{x}(t)$ in Sec. II, we further write (28) as

$$\langle\downarrow|\uparrow\rangle = \langle i|e^{-ik\hat{x}(t)}e^{ik\hat{x}(2t)}e^{-ik\hat{x}(t)}e^{ik\hat{x}}|i\rangle. \qquad (29)$$

In terms of $1/R$, the positional operator was perturbatively expanded as $\hat{x}(t) = \hat{x}_0(t) + \hat{x}_1(t)/R + \hat{x}_2(t)/R^2$. As a consequence, the exponent is expanded as

$$e^{-ik\hat{x}(t)} \approx e^{-ik\hat{x}_0(t)}\hat{L}(t,k,\hat{\mathbf{r}},\hat{\mathbf{v}}) \qquad (30)$$

by using the Zassenhaus formula. Here,

$$\hat{L}(t,k,\hat{\mathbf{r}},\hat{\mathbf{v}}) = e^{-i\frac{k\hat{x}_1}{R}}e^{\frac{k^2}{2R}[\hat{x}_0,\hat{x}_1]} \times e^{-i\frac{k\hat{x}_2}{R^2}}e^{\frac{k^2}{2R^2}[\hat{x}_0,\hat{x}_2]}$$
$$\times e^{i\frac{k^3}{6R^2}[\hat{x}_0,[\hat{x}_0,\hat{x}_2]]}, \qquad (31)$$

with

$$[\hat{x}_0,\hat{x}_1] = -\frac{2gt^3}{3}\frac{i\hbar}{m},$$

$$[\hat{x}_0,\hat{x}_2] = \left(2gt^3\hat{x} + \frac{gt^4}{2}\hat{v}_x - \frac{7g^2t^5}{30}\right)\frac{i\hbar}{m},$$

$$[\hat{x}_0,[\hat{x}_0,\hat{x}_2]] = \frac{3gt^4}{2}\frac{\hbar^2}{m^2}. \qquad (32)$$

In the above Zassenhaus formula, the terms with the higher orders than $1/R^2$ have been neglected, as well as that in Sec. II.

Using formula (30), the exponents product in formula (29) is written as

$$\hat{K} = e^{-ik\hat{x}(t)}e^{ik\hat{x}(2t)}e^{-ik\hat{x}(t)}e^{ik\hat{x}}$$
$$= e^{-ik\hat{x}_0(t)}\hat{L}(t,k,\hat{\mathbf{r}},\hat{\mathbf{v}})e^{ik\hat{x}_0(2t)}$$
$$\times \hat{L}(2t,-k,\hat{\mathbf{r}},\hat{\mathbf{v}})e^{-ik\hat{x}_0(t)}\hat{L}(t,k,\hat{\mathbf{r}},\hat{\mathbf{v}})e^{ik\hat{x}}$$
$$= \hat{L}(t,k,\hat{\mathbf{r}}-\hat{\mathbf{r}}_d,\hat{\mathbf{v}}+\hat{\mathbf{v}}_d)\hat{L}(2t,-k,\hat{\mathbf{r}}+\hat{\mathbf{r}}_d,\hat{\mathbf{v}})$$
$$\times \hat{L}(t,k,\hat{\mathbf{r}},\hat{\mathbf{v}}+\hat{\mathbf{v}}_d)e^{-igkt^2}. \qquad (33)$$

In the last line of the above equation, we have used the identities

$$e^{-ik\hat{x}_0(t)}\hat{\mathbf{v}}e^{ik\hat{x}_0(t)} = \hat{\mathbf{v}} + \hat{\mathbf{v}}_d, \qquad \hat{\mathbf{v}}_d = \frac{\hbar k}{m}(1,0,0), \qquad (34)$$

$$e^{-ik\hat{x}_0(t)}\hat{\mathbf{r}}e^{ik\hat{x}_0(t)} = \hat{\mathbf{r}} - \hat{\mathbf{r}}_d, \qquad \hat{\mathbf{r}}_d = t\hat{\mathbf{v}}_d. \qquad (35)$$

The first result from Eq. (33) is $\theta_0 = gkt^2$, the well-known phase of AI generated by the uniform gravity. If one neglects the corrections from the order $1/R^2$, Eq. (31) reduces to

$$\hat{L}_1 = e^{-i\frac{\theta_0}{R}(\hat{x}+\frac{1}{3}\hat{v}_xt)}e^{i\frac{\theta_0gt^2}{12R}}e^{-i\frac{\theta_0\hbar kt}{3mR}}. \qquad (36)$$

As a consequence, the operator $\hat{K}$ reduces to

$$\hat{K}_1 = e^{-i\frac{\theta_0}{R}(\hat{x}+\frac{\hat{v}_xt}{3})}e^{i\frac{4\theta_0}{R}(\hat{x}+\frac{2\hat{v}_xt}{3})}e^{-i\frac{\theta_0}{R}(\hat{x}+\frac{\hat{v}_xt}{3})}e^{-i(\theta'+\theta_0)}$$
$$= e^{i\frac{2\theta_0}{R}(\hat{x}+\hat{v}_xt)}e^{-i(\theta'+\theta_0)}, \qquad (37)$$

with

$$\theta' = \frac{7\theta_0gt^2}{6R} - \frac{\theta_0\hbar kt}{mR}. \qquad (38)$$

The phase θ' is due to the gravity gradient $2g/R$, and independent on the initial state $|i\rangle$ of the atom. In Refs. [23,24], there still exists a phase relating to the initial velocity of the atom. For that, we Taylor expand $\exp[i2\theta_0(\hat{x}+\hat{v}_xt)/R]$, and consequently,

$$\langle i|\hat{K}_1|i\rangle \approx \left[1 + i\frac{2\theta_0}{R}(\langle i|\hat{x}|i\rangle + t\langle i|\hat{v}_x|i\rangle)\right]e^{-i(\theta'+\theta_0)}. \quad (39)$$

Indeed, there is a phase $\theta_{v_x} = 2\theta_0 t\langle i|\hat{v}_x|i\rangle/R$ referring to the atomic initial central velocity $v_{xi} = \langle i|\hat{v}_x|i\rangle$ along the x-direction.

B. Phase shift due to the initial velocity uncertainty

In terms of $1/R$ and $1/R^2$, we write formula (31) as $\hat{L} = \hat{L}_1\hat{L}_2$, with

$$\hat{L}_2(t, k, \hat{\mathbf{r}}, \hat{\mathbf{v}}) = e^{-i\frac{k\hat{x}_2}{R^2}}e^{\frac{k^2}{2R^2}[\hat{x}_0, \hat{x}_2]}e^{i\frac{k^3}{6R^2}[\hat{x}_0, [\hat{x}_0, \hat{x}_2]]}. \quad (40)$$

Note that $[\hat{L}_1, \hat{L}_2] \approx 0$ and $[\hat{L}_2(t, k), \hat{L}_2(2t, -k)] \approx 0$, because the outcomes of such commutators are on the order of $1/R^3$. As a consequence, $\hat{K} \approx \hat{K}_1\hat{K}_2$, with

$$\begin{aligned}\hat{K}_2 &= \hat{L}_2(t, k, \hat{\mathbf{r}} - \hat{\mathbf{r}}_d, \hat{\mathbf{v}} + \hat{\mathbf{v}}_d)\hat{L}_2(2t, -k, \hat{\mathbf{r}} + \hat{\mathbf{r}}_d, \hat{\mathbf{v}}) \\ &\quad \times \hat{L}_2(t, k, \hat{\mathbf{r}}, \hat{\mathbf{v}} + \hat{\mathbf{v}}_d) \\ &\approx e^{i\frac{k}{R^2}[\hat{x}_2(2t) - 2\hat{x}_2(t)]}e^{i(\mu\hat{x} + \nu\hat{v}_x t)}e^{i\theta''}.\end{aligned} \quad (41)$$

Above, θ'' is a real number and independent on the initial state of the atom, as well as the standard phase shift θ_0 and θ' from the first-order gravity gradient. The μ and ν are the coefficients for the linear operators $\hat{x}$ and $\hat{v}_x$ in $\exp[i(\mu\hat{x} + \nu\hat{v}_x t)]$. This term generates a phase that depends on the central position and the central velocity of incident atoms, see Eq. (39).

In $\hat{K}_2$, the operator $\hat{x}_2(t)$ has been already solved in Sec. II, which contains the quadratic operators, such as $\hat{v}_x^2$. Thus, Taylor expanding the exponential operator in $\langle i|\hat{K}_1\hat{K}_2|i\rangle$, one can find that there exists a phase depending on the velocity uncertainty of incident state $|i\rangle$. This is one of the new systematic effects different from that of the first-order gravity gradient. For demonstrating such effect, one can apply an additional manipulation (before the standard AI) to change the initial momentum uncertainty of incident atoms but not change the central momentum and central position of the atomic wave packet. This manipulation can be realized by a pulse of standing-wave light which generates the atomic Kapitza-Dirac scattering [42–44]. The phase shift due to such an additional laser pulse along the x-direction is

$$\theta_{v_x^2} = \frac{7gkt^4}{2R^2}\langle i|\hat{v}_x^2|i\rangle. \quad (42)$$

Numerically, assuming $\sqrt{\langle i|\hat{v}_x^2|i\rangle} = 0.1\hbar k/m \approx 10^{-3}$ m/s with $k = 2\pi/(500 \text{ nm})$ and $m = 10^{-25}$ kg, we have $\theta_{v_x^2} \approx 5.9\pi \times 10^{-12}$ with $t = 1$ s. Here, $R \approx 6.4 \times 10^6$ m and $g = GM/R^2 \approx 9.8$ m/s^2 are respectively Earth's radius and the gravitational acceleration at Earth's surface. Compared to

the standard phase shift θ_0 and the θ_{v_x} of gravity gradient, the present phase shift is very small,

$$\frac{\theta_{v_x^2}}{\theta_0} = \frac{7t^2\langle i|\hat{v}_x^2|i\rangle}{2R^2} \ll \frac{\theta_{v_x^2}}{\theta_{v_x}} = \frac{7t\langle i|\hat{v}_x^2|i\rangle}{4R\langle i|\hat{v}_x|i\rangle} \ll 1, \quad (43)$$

because of large R and short t in the ground-based laboratory. However, the situation would be different in microgravity environments, for example, the gravity of a satellite in the space laboratory. Using the data $M = 10^3$ kg, $R = 1.5$ m, and $t = 10$ s in the paragraph below Eq. (2), we have $g = GM/R^2 \approx 3 \times 10^{-8}$ m/s^2, $\theta_0 \approx 12\pi$, and $\theta_{v_x^2} \approx 3.2\pi \times 10^{-3}$. The phase shifts get smaller linearly with decreasing M, for example, $\theta_0 \approx 1.2\pi$ and $\theta_{v_x^2} \approx 3.2\pi \times 10^{-4}$ with $M = 100$ kg. The background noises in space laboratory, such as the blackbody radiation and the seismic noise (the vibration of experimental platform) are much smaller than those in the ground-based laboratory. Therefore, the atomic coherent time $t = 10$ s or longer is possible [20,21].

C. Gravity simulation

For experimentally demonstrating the above effects in the ground-based laboratory, one can use electromagnetic force to simulate gravity. Consider a magnetic field, $\vec{B} = \vec{e}_n\mu_0I/[2\pi(R + x)]$, that is generated by a dc current $\vec{I}$ along the vertical direction. Here, μ_0 is the permeability of vacuum, $\vec{e}_n$ is the unit vector normal to the plane of I and $R + x$. Here, $R + x$ is the distance between the atom and current, and x is the dynamical position of the atom. Within the limitation $x \ll R$, the potential energy of the atom in the nonuniform magnetic field can be expanded as

$$\phi_b = -\frac{\mu_0IM_b}{2\pi(R + x)} \approx mg_bx - \frac{mg_b}{R}x^2 + \frac{mg_b}{R^2}x^3, \quad (44)$$

with M_b being the effective magnetic moment of the atom, and acceleration $g_b = \mu_0IM_b/(2\pi R^2 m)$. The present equation is very like the gravitational (1). The advantage is that the value of g_b/R^2 can be much larger than the gravitational counterpart. Numerically, supposing $R = 0.1$ m, $g_b = 0.1$ m/s^2, and $t = 0.1$ s, we have $\theta_0 \approx 4\pi \times 10^3$ and $\theta_{v_x^2} \approx 0.025\pi$, with the same values of m, k, and $\langle i|\hat{v}_x^2|i\rangle$ as before.

IV. NONCLASSICALITY IN TERMS OF WIGNER EQUATION

In Sec. III, quantum interference was obtained by applying several laser pulses to create a superposition state of atomic momentum via the help of atomic internal bound states. One might ask whether gravity itself generates the genuine nonclassicality regardless of laser manipulations. In this section, we discuss this issue based on the Wigner

equation, which was introduced first by Wigner in 1932 [35]. This equation is equivalent to the Schrödinger equation for the dynamical evolution of a pure state, and thus sometimes called Wigner equivalent formalism [45]. At the same time, this equation also works for the mix state [46,47]. The Wigner equation looks similar to the Newtonian equation in phase space and allows us to make an intuitive comparison between classical and quantum mechanics [48]. In terms of the Wigner equation, the quantum correction is on the order of $\hbar^2/m^2$, and the arose gravitational quantum effects are too weak to be experimentally demonstrated so far.

A. Wigner function

Without generality, we start with the Wigner function in spatial 3-dimensions. It is defined as [35]

$$W(\mathbf{r},\mathbf{p},t) = \frac{1}{(2\pi\hbar)^3} \int_{-\infty}^{\infty} e^{i\mathbf{p}\cdot\mathbf{r}'/\hbar} \psi^*(\mathbf{r}+\mathbf{r}'/2,t)$$
$$\times \psi(\mathbf{r}-\mathbf{r}'/2,t)\mathrm{d}^3 r', \qquad (45)$$

with $\psi(\mathbf{r},t)$ being the time-dependent state of a quantum system, and where $\mathbf{r} = (x,y,z)$ and $\mathbf{p} = (p_x,p_y,p_z)$. Following this definition, any observable quantity of the system can be formally written as [48]

$$\langle\psi|\hat{O}|\psi\rangle = \int_{-\infty}^{\infty} \tilde{O}W(\mathbf{r},\mathbf{p},t)\mathrm{d}^3 r \mathrm{d}^3 p, \qquad (46)$$

with

$$\tilde{O} = \int_{-\infty}^{\infty} e^{-i\mathbf{p}\cdot\mathbf{r}'/\hbar}\langle\mathbf{r}+\mathbf{r}'/2|\hat{O}|\mathbf{r}-\mathbf{r}'/2\rangle\mathrm{d}^3 r' \qquad (47)$$

being the so-called Weyl transform of a Hermitian operator $\hat{O}$. In this representation, the observable quantity $\tilde{O}$ is a function of $\mathbf{r}$ and $\mathbf{p}$, not the function of operators $\hat{\mathbf{r}}$ and $\hat{\mathbf{p}}$.

It has been well known: $\int_{-\infty}^{\infty} W(\mathbf{r},\mathbf{p},t)\mathrm{d}^3 p \mathrm{d}^3 r = 1$, $|\psi(\mathbf{r},t)|^2 = \int_{-\infty}^{\infty} W(\mathbf{r},\mathbf{p},t)\mathrm{d}^3 p$, and $|\varphi(\mathbf{p},t)|^2 = \int_{-\infty}^{\infty} W(\mathbf{r},\mathbf{p},t)\mathrm{d}^3 r$ with $\varphi(\mathbf{p},t)$ being the wave function in momentum Hilbert space of state $\psi(\mathbf{r},t)$. Moreover, if $\hat{O}$ is purely a function of $\hat{x}$ or $\hat{p}_x$, then its Weyl transform is just the original function [48], i.e., $\widetilde{x^n} = x^n$ and $\widetilde{p_x^n} = p_x^n$, with $n = 0,1,2,\ldots$. Consequently, $\langle x\rangle = \int_{-\infty}^{\infty} xW(\mathbf{r},\mathbf{p},t)\mathrm{d}^3 r \mathrm{d}^3 p$, $\langle x^2\rangle = \int_{-\infty}^{\infty} x^2 W(\mathbf{r},\mathbf{p},t)\mathrm{d}^3 r \mathrm{d}^3 p$, etc. The y- and z-directional formulas take the similar forms. Because these representations are the same as the classical statistics in phase space, the Wigner function is also called Wigner quasiprobability distribution. Note that the Weyl transform of $\hat{x}\hat{p}_x + \hat{p}_x\hat{x}$ is also its original function, i.e., $\widetilde{xp_x} + \widetilde{p_x x} = 2xp_x$. Hence, the position or momentum average with the given Heisenberg operator (19) in Sec. II can be regarded as a classical measurement to the initial Wigner function $W(\mathbf{r},\mathbf{p},0)$. However, the results

would be different for some other measurable quantities, such as the distribution function $|\psi(\mathbf{r},t)|^2$ in real space. Thus, it is necessary to study the time-dependent Wigner function $W(\mathbf{r},\mathbf{p},t)$.

B. Wigner equation with lowest-order quantum correction

The time evolution of wave function $\psi(\mathbf{r},t)$ obeys the Schrödinger equation, and thus one can establish a dynamical equation for the Wigner function, with definition (45) and the Hamiltonian $\hat{H} = \hat{\mathbf{p}}^2/(2m) + V(\mathbf{r})$. Solving the original $(6+1)$-dimensional Wigner equation is a huge challenge [46,47], especially with the present central force problem. Nevertheless, it is resolvable within the classical limitation $\hbar^2 \to 0$ [49–51]. In such a limitation, the Wigner equation reads [46]

$$\partial_t W(\mathbf{r},\mathbf{p},t) + \frac{\mathbf{p}}{m}\cdot\nabla_r W(\mathbf{r},\mathbf{p},t) - \nabla_r V(\mathbf{r})\cdot\nabla_p W(\mathbf{r},\mathbf{p},t) = Q, \qquad (48)$$

with

$$Q = \frac{-\hbar^2}{24}\nabla_r^3 V(\mathbf{r})\cdot\nabla_p^3 W(\mathbf{r},\mathbf{p},t) + \mathcal{O}(\hbar^2), \qquad (49)$$

where $\nabla_r = (\partial_x,\partial_y,\partial_z)$ and $\nabla_p = (\partial_{p_x},\partial_{p_y},\partial_{p_z})$. The $\hbar^2$-dependent Q can be regarded as a quantum mechanical correction to the dynamical system, because if $Q = 0$, Eq. (48) is exactly the classical Liouville equation. In Eq. (49), the high orders of $\hbar^2$ have been neglected. This approximation was numerically verified by many previous references for the one-dimensional questions, see, e.g., [49–51]. In terms of velocity $\mathbf{v} = \mathbf{p}/m$ and acceleration $\mathbf{g}(\mathbf{r}) = -\nabla_r V(\mathbf{r})/m = -\nabla_r\phi(\mathbf{r})$, the Wigner equation can be further written as

$$\partial_t f(\mathbf{r},\mathbf{v},t) + \mathbf{v}\cdot\nabla_r f(\mathbf{r},\mathbf{v},t) + \mathbf{g}(\mathbf{r})\cdot\nabla_v f(\mathbf{r},\mathbf{v},t) = Q, \qquad (50)$$

with $\nabla_v = (\partial_{v_x},\partial_{v_y},\partial_{v_z})$. Using our approximate potential (1), the quantum correction reads

$$Q \approx \varepsilon_q\left(\frac{3}{2}\partial_{v_y}^2 + \frac{3}{2}\partial_{v_z}^2 - \partial_{v_x}^2\right)\partial_{v_x} f(\mathbf{r},\mathbf{v},t), \qquad (51)$$

with

$$\varepsilon_q = \frac{g\hbar^2}{4R^2 m^2} = \frac{GM\hbar^2}{4R^4 m^2}. \qquad (52)$$

Correspondingly, the function $f(\mathbf{r},\mathbf{v},t)$ can be regarded as a quasiprobability distribution in the phase space of position and velocity, with $P(\mathbf{r},t) = \int_{-\infty}^{\infty} f(\mathbf{r},\mathbf{v},t)\mathrm{d}^3 v$ being a measurable probability distribution in real space. With the given acceleration $\mathbf{g}(\mathbf{r})$, the distribution function

$f(\mathbf{r}, \mathbf{v}, t)$ and its consequence $P(\mathbf{r}, t)$ depend on mass m of test particles. This is obviously a nonclassical phenomenon. Note that Q decreases with increasing mass, the corresponding principle holds. This guarantees the validity of the above semiclassical approximation. One can find that the neglected terms in the original Wigner equation are relating to the high orders of small-quantity $\hbar^2/m^2$. The nonzero Q requires that third and higher derivatives of $V(\mathbf{r})$ are nonzero. Thus, for the linear or quadric potential, the Wigner equation takes the same form as the classical Liouville equation. Nevertheless, we cannot conclude that the states within linear or quadratic potential are classical, because the initial states can be prepared in nonclassical states whose Wigner functions have negative values, for example, the well-known Fock state $|n\rangle$ (with $n \geq 1$) of harmonic oscillator [52,53]. Finally, we would like to emphasize that the Wigner equation (50) holds also for the two-body motion, where the variables $\mathbf{r}$ and $\mathbf{v}$ are respectively the relative position and relative velocity between two gravitationally interacting objects (of masses m_1 and m_2). The quantum correction is $\varepsilon_q^d = \hbar^2 G M^3/(4R^4 m_1^2 m_2^2)$ with total mass $M = m_1 + m_2$ and the reduced mass $m_1 m_2/(m_1 + m_2)$. The ε_q^d can reduce to (52) with $m_1 \gg m_2$.

C. The perturbation solution

In short, we rewrite the Wigner equation (50) as

$$\partial_t f = -(\hat{L} - \varepsilon_q \hat{L}_q)f, \tag{53}$$

with the classical Liouville operator

$$\hat{L} = \mathbf{v} \cdot \nabla_r + \mathbf{g}(\mathbf{r}) \cdot \nabla_v, \tag{54}$$

and a quantum correction

$$\hat{L}_q = \left(\frac{3}{2}\partial_{v_y}^2 + \frac{3}{2}\partial_{v_z}^2 - \partial_{v_x}^2\right)\partial_{v_x}. \tag{55}$$

Similar to the solution of the Schrödinger equation in an interacting picture, we formally write the solution of Eq. (53) as

$$f = e^{-t\hat{L}}f', \tag{56}$$

with

$$\partial_t f' = \varepsilon_q e^{t\hat{L}}\hat{L}_q e^{-t\hat{L}}f'$$
$$\approx \varepsilon_q e^{t\hat{L}_0}\hat{L}_q e^{-t\hat{L}_0}f', \tag{57}$$

and where

$$\hat{L}_0 = v_x\partial_x + v_y\partial_y + v_z\partial_z - g\partial_{v_x} \tag{58}$$

is just the Liouville operator with constant gravitational acceleration g. For deriving the first line in (57), we have used the relation $\exp(t\hat{L})\exp(-t\hat{L}) = 1$, which can be easily proved by the Zassenhaus formula (24) in Sec. III. In the second line of (57), the gradient gravity in the exponential operator has been neglected, because ε_q is already a small quantity. This approximation will greatly simplify our subsequent derivations.

Integrating Eq. (57) and neglecting the high orders of ε_q^2, we have

$$f'(\mathbf{r}, \mathbf{v}, t) = f'(\mathbf{r}, \mathbf{v}, 0) + \varepsilon_q \int_0^t e^{\tau\hat{L}_0}\hat{L}_q e^{-\tau\hat{L}_0}f'(\mathbf{r}, \mathbf{v}, \tau)d\tau$$

$$\approx f'(\mathbf{r}, \mathbf{v}, 0) + \varepsilon_q \int_0^t e^{\tau\hat{L}_0}\hat{L}_q e^{-\tau\hat{L}_0}d\tau f'(\mathbf{r}, \mathbf{v}, 0)$$

$$+ \mathcal{O}(\varepsilon_q^2). \tag{59}$$

As a consequence, the Wigner function is solved as

$$f(\mathbf{r}, \mathbf{v}, t) \approx e^{-t\hat{L}}f'(\mathbf{r}, \mathbf{v}, 0) + \varepsilon_q \hat{D}e^{-t\hat{L}_0}f'(\mathbf{r}, \mathbf{v}, 0)$$
$$= f_c(\mathbf{r}, \mathbf{v}, t) + \varepsilon_q \hat{D}f_u(\mathbf{r}, \mathbf{v}, t)$$
$$= f_c(\mathbf{r}, \mathbf{v}, t) + f_q(\mathbf{r}, \mathbf{v}, t), \tag{60}$$

with

$$\hat{D}(t) = \int_0^t e^{(\tau-t)\hat{L}_0}\hat{L}_q e^{-(\tau-t)\hat{L}_0}d\tau$$

$$= \int_{-t}^0 e^{\tau\hat{L}_0}\hat{L}_q e^{-\tau\hat{L}_0}d\tau$$

$$= \int_{-t}^0 \hat{S}(\tau)d\tau. \tag{61}$$

In Eq. (60), $f_c(\mathbf{r}, \mathbf{v}, t) = \exp(-t\hat{L})f(\mathbf{r}, \mathbf{v}, 0)$ and $f_u(\mathbf{r}, \mathbf{v}, t) = \exp(-t\hat{L}_0)f(\mathbf{r}, \mathbf{v}, 0)$ are the solutions of classical Liouville equations with nonuniform and the uniform gravitational accelerations, respectively. The quantum mechanical correction $f_q(\mathbf{r}, \mathbf{v}, t) = \varepsilon_q \hat{D}f_u(\mathbf{r}, \mathbf{v}, t)$ is equal to zero at the initial time $t = 0$, so that $f_q(\mathbf{r}, \mathbf{v}, t)$ is not the correction for the initial state but a dynamical one.

The integral kernel $\hat{S}(\tau) = \exp(\tau\hat{L}_0)\hat{L}_q\exp(-\tau\hat{L}_0)$ in (61) can be computed by using BCH formula (25) in Sec. III. We have

$$e^{\tau\hat{L}_0}\partial_{v_x}e^{-\tau\hat{L}_0} = \partial_{v_x} + \tau[\hat{L}_0, \partial_{v_x}] = \partial_{v_x} - \tau\partial_x, \tag{62}$$

and consequently

$$e^{\tau\hat{L}_0}\partial_{v_x}^2 e^{-\tau\hat{L}_0} = e^{\tau\hat{L}_0}\partial_{v_x}e^{-\tau\hat{L}_0}e^{\tau\hat{L}_0}\partial_{v_x}e^{-\tau\hat{L}_0}$$
$$= (\partial_{v_x} - \tau\partial_x)^2. \tag{63}$$

These formulas can be directly generalized into y- and z-directions, and thus

$$\hat{S}(\tau) = \frac{3}{2}(\partial_{v_y} - \tau\partial_y)^2(\partial_{v_x} - \tau\partial_x)$$

$$+ \frac{3}{2}(\partial_{v_z} - \tau\partial_z)^2(\partial_{v_x} - \tau\partial_x) - (\partial_{v_x} - \tau\partial_x)^3. \quad (64)$$

Operator (64) includes many terms, so that solving the quantum correction $f_q(\mathbf{r}, \mathbf{v}, t) = \varepsilon_q \int_{-t}^{0} \hat{S}(\tau)f_u(\mathbf{r}, \mathbf{v}, t)d\tau$ is still very complex. However, it is easy to solve the quantum correction in one-dimensional real space, for example,

$$P_q(x, t) = \int_{-\infty}^{\infty} f_q(\mathbf{r}, \mathbf{v}, t)d^3 v dy dz$$

$$= \varepsilon_q \int_{-t}^{0}\int_{-\infty}^{\infty} \hat{S}(\tau)f_u(\mathbf{r}, \mathbf{v}, t)d^3 v dy dz d\tau$$

$$= -\frac{\varepsilon_q t^4}{4}\partial_x^3\int_{-\infty}^{\infty} f_u(\mathbf{r}, \mathbf{v}, t)d^3 v dy dz$$

$$= -\frac{\varepsilon_q t^4}{4}\partial_x^3 P_u(x, t). \quad (65)$$

In the third line of the above equation, we have used the locality of classical particles ensemble,

$$\lim_{\eta\to\pm\infty} f_u(\mathbf{r}, \mathbf{v}, t) = \lim_{\eta\to\pm\infty} [\partial_\eta f_u(\mathbf{r}, \mathbf{v}, t)]$$

$$= \lim_{\eta\to\pm\infty} [\partial_\eta^2 f_u(\mathbf{r}, \mathbf{v}, t)] = 0, \quad (66)$$

with η being one of the variables (x, y, z, v_x, v_y, v_z), and thus $\int_{-\infty}^{\infty}(\partial_\eta f_u)d\eta = \int_{-\infty}^{\infty}(\partial_\eta^2 f_u)d\eta = \int_{-\infty}^{\infty}(\partial_\eta^3 f_u)d\eta = 0$. In the last line of Eq. (65), $P_u(x, t) = \int_{-\infty}^{\infty} f_u(\mathbf{r}, \mathbf{v}, t)d^3 v dy dz$ is the one-dimensional probability distribution with constant acceleration. For the same reason, $\int_{-\infty}^{\infty} P_q(x, t)dx = 0$, so that the total probability is conserved [the classical distribution f_c in Eq. (60) is already normalized].

Note that Eq. (65) can be proved by directly applying the Weyl transform to the already obtained Heisenberg operator $\hat{x}(t)$ in Sec. II. The Weyl transforms of $\hat{x}(t)$ and $\hat{x}(t)^2$ are their original functions, so that $\langle i|\hat{x}(t)|i\rangle$ and $\langle i|\hat{x}(t)^2|i\rangle$ evolve classically. This means that the above $P_q(x, t)$ does not contribute to the average values of position and its square, i.e., $\int_{-\infty}^{\infty} x\partial_x^3 P_u dx = \int_{-\infty}^{\infty} x^2\partial_x^3 P_u dx = 0$. This can be proved by expanding the integrands as the forms of first-order derivation: $x\partial_x^3 P_u = \partial_x(x\partial_x^2 P_u - \partial_x P_u)$, $x^2\partial_x^3 P_u = \partial_x(x^2\partial_x^2 P_u - 2x\partial_x P_u + 2P_u)$. The functions in the round brackets are convergent at $x\to\pm\infty$ for any local distribution P_u. In fact, the above zero result can be also proved by using the Dirac delta function. Writing $P_u(x, t) = \int_{-\infty}^{\infty} P_u(x', t)\delta(x - x')dx'$, we have $\int_{-\infty}^{\infty} x^n\partial_x^3 P_u(x, t)dx = \int_{-\infty}^{\infty}\int_{-\infty}^{\infty} P_u(x', t)x^n\partial_x^3\delta(x - x')dxdx' = -\int_{-\infty}^{\infty} P_u(x', t)\times(\partial_{x'}^3 x'^n)dx'$, with $n = 0, 1, 2, 3$. Immediately, we see $\int_{-\infty}^{\infty} x^3\partial_x^3 P_u dx = -6$, i.e., the quantum correction should contribute the average value of x^3. This is true, and can be also proved by the Weyl transform of cubic operator $\hat{x}(t)^3$.

Using formula (19) in Sec. II, one can find $\hat{x}(t)^3$ containing $\hat{x}^2\hat{v}_x^2 + \hat{v}_x^2\hat{x}^2$, $\hat{x}\hat{v}_x^2\hat{x}$, $\hat{v}_x\hat{x}^2\hat{v}_x$, and $(\hat{x}\hat{v}_x + \hat{v}_x\hat{x})^2$, whose Weyl transforms are not their original functions [48].

D. The tiny quantum fluctuation

The quantum correction $P_q(x, t)$ is now resolvable based on the given classical probability density $P_u(x, t) = \int_{-\infty}^{\infty} f_u(\mathbf{r}, \mathbf{v}, t)d^3 v dy dz$ in the uniform gravitational field, where the integrand can be easily computed by the classical trajectory-dynamics method [54],

$$f_u(x, v_x, t) = \int_{-\infty}^{\infty} \delta[x - (x_i + v_{xi}t - gt^2/2), v_x - (v_{xi} - gt)]$$

$$\times f(x_i, v_{xi}, 0)dx_i dv_{xi}$$

$$= f_u(x - v_x t - gt^2/2, v_x + gt). \quad (67)$$

In short, the variables in y- and z-directions are not written, and $f(x_i, v_{xi}, 0)$ is the probability of particles that are initially at position x_i and velocity v_{xi}. Supposing the initial Wigner function takes Gaussian form [36]

$$f(x, v_x, 0) = \frac{1}{2\pi\sigma_x\sigma_v}\exp\left[-\frac{x^2}{2\sigma_x^2} - \frac{v_x^2}{2\sigma_v^2}\right], \quad (68)$$

with the standard deviations σ_x and σ_v. According to Eq. (67), replacing x by $x - v_x t - gt^2/2$, and v_x by $v_x + gt$, the above initial state becomes the desired time-dependent state $f_u(x, v_x, t)$. Consequently, using the Gaussian integral we have

$$P_u(x, t) = \int_{-\infty}^{\infty} f_u(x, v_x, t)dv_x$$

$$= \frac{1}{\sqrt{2\pi}\sqrt{\sigma_x^2 + \sigma_v^2 t^2}}\exp\left[-\frac{1}{2}\xi^2(x, t)\right], \quad (69)$$

with

$$\xi(x, t) = \frac{x + \frac{1}{2}gt^2}{\sqrt{\sigma_x^2 + \sigma_v^2 t^2}}. \quad (70)$$

Finally, quantum probability density (65) is given as

$$P_q(x, t) = P_0\frac{t^4[\xi^3(x, t) - 3\xi(x, t)]}{[(\sigma_x/\sigma_v)^2 + t^2]^2\sqrt{2\pi}}\exp\left[-\frac{1}{2}\xi^2(x, t)\right], \quad (71)$$

with

$$P_0 = \frac{g\hbar^2}{16R^2 m^2\sigma_v^4}. \quad (72)$$

Figure 3 shows that $P_q(x, t)$ is positive in some regions and negative in others. The previous arguments $\int_{-\infty}^{\infty} P_q(x, t)dx = 0$ etc. can be also proved by the numerical integrals of (71). The P_0 is the characteristic probability density, which increases rapidly with the decreasing of
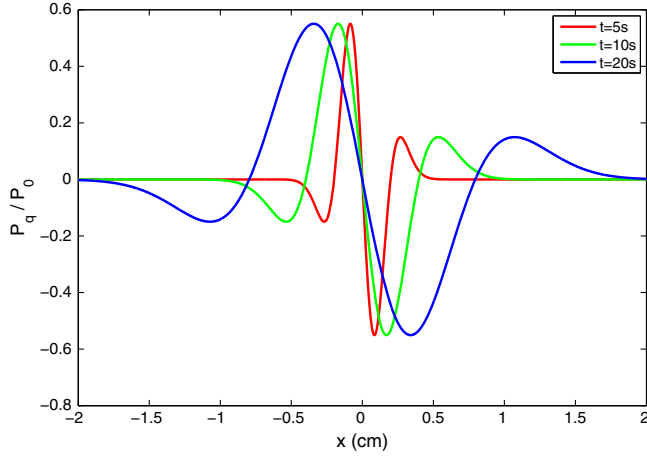
FIG. 3. Quantum fluctuation in one-dimensional real space, with $R = 1.5$ m, $M = 10^3$ kg, $m = 10^{-25}$ kg, $\sigma_x \approx 3$ μm, and $\sigma_v \approx 3 \times 10^{-4}$ m/s.

velocity uncertainty, as $1/\sigma_v^4$. Thus, the cooled neutral atom may be appropriate for achieving a relatively large value of P_0. Consider an atom (of mass m) is initially confined in an optical trap as a harmonic oscillator (of frequency ω) and laser cooled in its vibrational ground state. Removing instantaneously the optical trapping, the atom is released as a freely falling body. The position and velocity uncertainties of the initial wave packet are on the orders of $\sigma_x = \sqrt{\hbar/(2m\omega)} \approx 3$ μm and $\sigma_v = \sqrt{\hbar\omega/(2m)} \approx 0.3$ mm/s, if $m \approx 10^{-25}$ kg and $\omega \approx 100$ Hz [55,56]. For the term $g/R^2 = GM/R^4$, we still consider $R = 1.5$ m and $M = 10^3$ kg as before, and thus $P_0 \approx 3.3 \times 10^{-13}$ per meter. This is a very small probability density, beyond the experimental ability. Assuming $\sigma_v \approx 2.3$ μm/s and $\sigma_x \approx 0.23$ mm of $\omega = 0.01$ Hz (not the experimental data), then P_0 is significantly enlarged to $P_0 \approx 3.3 \times 10^{-5}$ per meter.

One may notice $P_0 \propto 1/m^2$ and thus electrons should have significant quantum effects. This is true and can be found in the hydrogen atom. If we replace electronic mass by an atomic mass and retain Coulomb potential unchanging, then the separateness of the Bohr radius is not obvious. However, using electron as a free fall to measure gravity is impractical, because it is very sensitive to the electromagnetic noise. Thus, the key technologies for quantum free fall experiments are atom cooling and noises shielding. Finally, we emphasize that P_q is still not the final result. The true probability density is $P = P_c + P_q$, see Eq. (60). The classical part P_c may be numerically solved by the computer command of conditional sum: $P_c(x,t) = \prod_j \sum_{n_j} f(\mathbf{r}_d, \mathbf{v}_d, 0)(\Delta x)^2 (\Delta v)^3$, if $x \leq X(\mathbf{r}_d, \mathbf{v}_d, t) \leq x + \Delta x$. Here, $f(\mathbf{r}_d, \mathbf{v}_d, 0)$ is the initial distribution function with the discretized position $\mathbf{r}_d = (n_1, n_2, n_3)\Delta x$ and velocity $\mathbf{v}_d = (n_4, n_5, n_6)\Delta v$, and $X(\mathbf{r}_d, \mathbf{v}_d, t)$ is the numerical solution of the Newtonian equation (15), with any initial

position $\mathbf{r}_d$ and initial velocity $\mathbf{v}_d$. As mentioned before, if one neglects the present term P_q, there still exists quantum phenomena in P_c (such as the familiar double-slit interference of matter waves in flat spacetime), because the initial state $f(\mathbf{r}_d, \mathbf{v}_d, 0)$ can be nonclassical. Hence, a more precise statement for $P_c(x, t)$ is that it can be solved by the classical trajectory with any given initial Wigner function.

V. CONCLUSION

We have studied the free fall of microparticles with high-order gravity gradients. It is shown that the cubic terms in the Newtonian potential shall generate a new phase shift in AI, which depends on the position and velocity uncertainties of the incident atoms. Certainly, this effect is negligible in the ground-based laboratory, because Earth's radius is far larger than atomic freely falling length limited by the practical vacuum installation. However, the present effect may be considerable in the space laboratory due to the gravity of the satellite. On the one hand, the size of the satellite is far smaller than Earth. On the other hand, the freely falling time can be very long within the microgravity system. Thus, this study may be useful for designing the high-precision AIs of avoidable systematic effects of nonlinear gravity. For the sake of economy, we also suggested using the force of atom moving in the nonuniform magnetic field to simulate the nonlinear gravity in the ground-based laboratory.

Another value of the present study, which is purely theoretical, refers to the nonclassicality of freely falling particles. With the presence of high-order gravity gradients, there exists a quantum correction in the dynamical equation of the Wigner function. Certainly, its contribution to the observable value is very tiny and has less feasibility in the current experiments. Nevertheless, we have learned that the nonclassicality of free fall refers two aspects. One is the initial state which can be nonclassical, prepared by the nongravity interaction. The other is the quantum-corrected dynamical equation regardless of initial state. The two aspects are both mass dependent. Thus, the freely falling microparticles should be mass dependent in general. As mentioned earlier, this is just a quantum mechanical effect, not EP violation. On the one hand, the dynamical equations throughout the paper are built on the principle that inertia mass is equal to gravitational mass. On the other hand, the gravitational Wigner equation satisfies the corresponding principle that the quantum correction vanishes with the increasing mass of test particles. Hence, the present violation of the universality of free fall is just a quantum mechanical effect of microparticles, not macroparticles.

[1] R. Colella, A. W. Overhauser, and S. A. Werner, Observation of Gravitationally Induced Quantum Interference, Phys. Rev. Lett. **34,** 1472 (1975).

[2] M. Kasevich and S. Chu, Measurement of the gravitational acceleration of an atom with a light-pulse atom interferometer, Appl. Phys. B **54,** 321 (1992).

[3] A. Peters, K. Y. Chung, and S. Chu, Measurement of gravitational acceleration by dropping atoms, Nature (London) **400,** 849 (1999).

[4] H. Müller, A. Peters, and S. Chu, A precision measurement of the gravitational redshift by the interference of matter waves, Nature (London) **463,** 926 (2010).

[5] C. W. Chou, D. B. Hume, T. Rosenband, and D. J. Wineland, Optical clocks and relativity, Science **329,** 1630 (2010).

[6] S. B. Koller, J. Grotti, St. Vogt, A. Al-Masoudi, S. Dörscher, S. Häfner, U. Sterr, and Ch. Lisdat, Transportable Optical Lattice Clock with 7×10^{-17} Uncertainty, Phys. Rev. Lett. **118,** 073601 (2017).

[7] A. D. Ludlow, M. M. Boyd, J. Ye, E. Peik, and P. O. Schmidt, Optical atomic clocks, Rev. Mod. Phys. **87,** 637 (2015).

[8] V. V. Nesvizhevsky et al., Quantum states of neutrons in the Earth's gravitational field, Nature (London) **415,** 297 (2002).

[9] T. Jenke, P. Geltenbort, H. Lemmel, and H. Abele, Realization of a gravity-resonance-spectroscopy technique, Nat. Phys. **7,** 468 (2011).

[10] G. Ichikawa et al., Observation of the Spatial Distribution of Gravitationally Bound Quantum States of Ultracold Neutrons and Its Derivation Using the Wigner Function, Phys. Rev. Lett. **112,** 071101 (2014).

[11] S. Fray, C. A. Diez, T. W. Hänsch, and M. Weitz, Atomic Interferometer with Amplitude Gratings of Light and Its Applications to Atom Based Tests of the Equivalence Principle, Phys. Rev. Lett. **93,** 240404 (2004).

[12] G. Rosi, G. D'Amico, L. Cacciapuoti, F. Sorrentino, M. Prevedelli, M. Zych, Č. Brukner, and G. M. Tino, Quantum test of the equivalence principle for atoms in coherent superposition of internal energy states, Nat. Commun. **8,** 15529 (2017).

[13] J.-P. Uzan, The fundamental constants and their variation: Observational and theoretical status, Rev. Mod. Phys. **75,** 403 (2003).

[14] S. Hossenfelder, Minimal length scale scenarios for quantum gravity, Living Rev. Relativity **16,** 2 (2013).

[15] J. Bergé, P. Brax, G. Métris, M. Pernot-Borràs, P. Touboul, and J.-P. Uzan, MICROSCOPE Mission: First Constraints on the Violation of the Weak Equivalence Principle by a Light Scalar Dilaton, Phys. Rev. Lett. **120,** 141101 (2018).

[16] B. Altschul et al., Quantum tests of the Einstein equivalence principle with the STE-QUEST space mission, Adv. Space Res. **55,** 501 (2015).

[17] W. Ertmer et al., Matter wave explorer of gravity (MWXG), Exp. Astron. **23,** 611 (2009).

[18] S. Schiller et al., Einstein gravity explorer—A medium-class fundamental physics mission, Exp. Astron. **23,** 573 (2009).

[19] G. M. Tino et al., Precision gravity tests with atom interferometry in space, Nucl. Phys. (Proc. Suppl.) **243**–**244B,** 203 (2013).

[20] J. Williams, S. Chiow, N. Yu, and H. Müller, Quantum test of the equivalence principle and space-time aboard the International Space Station, New J. Phys. **18,** 025018 (2016).

[21] D. N. Aguilera et al., STE-QUEST—Test of the universality of free fall using cold atom interferometry, Classical Quantum Gravity **31,** 115010 (2014).

[22] A. Peters, K. Y. Chung, and S. Chu, High-precision gravity measurements using atom interferometry, Metrologia **38,** 25 (2001).

[23] K. Bongs, R. Launay, and M. A. Kasevich, High-order inertial phase shifts for time-domain atom interferometers, Appl. Phys. B **84,** 599 (2006).

[24] P. Asenbaum, C. Overstreet, T. Kovachy, D. D. Brown, J. M. Hogan, and M. A. Kasevich, Phase Shift in an Atom Interferometer due to Spacetime Curvature across its Wave Function, Phys. Rev. Lett. **118,** 183602 (2017).

[25] A. M. Nobili, Fundamental limitations to high-precision tests of the universality of free fall by dropping atoms, Phys. Rev. A **93,** 023617 (2016).

[26] A. Roura, Circumventing Heisenberg's Uncertainty Principle in Atom Interferometry Tests of the Equivalence Principle, Phys. Rev. Lett. **118,** 160401 (2017).

[27] G. D'Amico, G. Rosi, S. Zhan, L. Cacciapuoti, M. Fattori, and G. M. Tino, Canceling the Gravity Gradient Phase Shift in Atom Interferometry, Phys. Rev. Lett. **119,** 253201 (2017).

[28] S. W. Chiow, J. Williams, N. Yu, and H. Müller, Gravity-gradient suppression in spaceborne atomic tests of the equivalence principle, Phys. Rev. A **95,** 021603(R) (2017).

[29] D. Greenberger, The role of equivalence in quantum mechanics, Ann. Phys. (Leipzig) **47,** 116 (1968).

[30] D. M. Greenberger, The disconnect between quantum mechanics and gravity, arXiv:1011.3719.

[31] A. Accioly and R. Paszko, Quantum mechanics versus equivalence principle, Phys. Rev. D **78,** 064002 (2008).

[32] M. M. Ali, A. S. Majumdar, D. Home, and A. K. Pan, On the quantum analogue of Galileo's leaning tower experiment, Classical Quantum Gravity **23,** 6493 (2006).

[33] L. Viola and R. Onofrio, Testing the equivalence principle through freely falling quantum objects, Phys. Rev. D **55,** 455 (1997).

[34] S. K. Foong, From Moon-fall to motions under inverse square laws, Eur. J. Phys. **29,** 987 (2008).

[35] E. Wigner, On the quantum correction for thermodynamic equilibrium, Phys. Rev. **40,** 749 (1932).

[36] A. González-Arroyo and F. Nuevo, Real-time quantum evolution in the classical approximation and beyond, Phys. Rev. D **86,** 103504 (2012).

[37] P. Storey and C. Cohen-Tannoudji, The Feynman path integral approach to atomic interferometry. A tutorial, J. Phys. II (France) **4,** 1999 (1994).

[38] S. Dimopoulos, P. W. Graham, J. M. Hogan, and M. A. Kasevich, General relativistic effects in atom interferometry, Phys. Rev. D **78,** 042003 (2008).

[39] P. Wolf, L. Blanchet, C. J. Bordé, S. Reynaud, C. Salomon, and C. Cohen-Tannoudji, Does an atom interferometer test the gravitational redshift at the Compton frequency?, Classical Quantum Gravity **28,** 145017 (2011).

[40] F. Casas, A. Murua, and M. Nadinic, Efficient computation of the Zassenhaus formula, Comput. Phys. Commun. **183,** 2386 (2012).

[41] R. M. Wilcox, Exponential operators and parameter differentiation in quantum physics, J. Math. Phys. (N.Y.) **8**, 962 (1967).

[42] S. Gupta, A. E. Leanhardt, A. D. Cronin, and D. E. Pritchard, Coherent manipulation of atoms with standing light waves, C. R. Acad. Sci. Paris Ser. IV **2**, 479 (2001).

[43] M. Zhang, Weak values obtained from mass-energy equivalence, Phys. Rev. A **95**, 012114 (2017).

[44] R. E. Sapiro, R. Zhang, and G. Raithel, Atom interferometry using Kapitza-dirac scattering in a magnetic trap, Phys. Rev. A **79**, 043630 (2009).

[45] E. J. Heller, Wigner phase space method: Analysis for semiclassical applications, J. Chem. Phys. **65**, 1289 (1976).

[46] J. M. Sellier, M. Nedjalkov, and I. Dimov, An introduction to applied quantum mechanics in the Wigner Monte Carlo formalism, Phys. Rep. **577**, 1 (2015).

[47] S. Solórzano, M. Mendoza, S. Succi, and H. J. Herrmann, Lattice Wigner equation, Phys. Rev. E **97**, 013308 (2018).

[48] W. B. Case, Wigner functions and Weyl transforms for pedestrians, Am. J. Phys. **76**, 937 (2008).

[49] H. W. Lee, Theory and application of the quantum phase-space distribution functions, Phys. Rep. **259**, 147 (1995).

[50] H. W. Lee and M. O. Scully, Wigner phase-space description of a Morse oscillator, J. Chem. Phys. **77**, 4604 (1982).

[51] A. Donoso and C. C. Martens, Quantum Tunneling Using Entangled Classical Trajectories, Phys. Rev. Lett. **87**, 223202 (2001).

[52] D. Leibfried, D. M. Meekhof, B. E. King, C. Monroe, W. M. Itano, and D. J. Wineland, Experimental Determination of the Motional Quantum State of a Trapped Atom, Phys. Rev. Lett. **77**, 4281 (1996).

[53] D. M. Meekhof, C. Monroe, B. E. King, W. M. Itano, and D. J. Wineland, Generation of Nonclassical Motional States of a Trapped Atom, Phys. Rev. Lett. **76**, 1796 (1996).

[54] C. Y. Wong, Dynamics of nuclear fluid. VIII. Time-dependent Hartree-Fock approximation from a classical point of view, Phys. Rev. C **25**, 1460 (1982).

[55] S. Bernon, H. Hattermann, D. Bothner, M. Knufinke, P. Weiss, F. Jessen, D. Cano, M. Kemmler, R. Kleiner, D. Koelle, and J. Fortágh, Manipulation and coherence of ultra-cold atoms on a superconducting atom chip, Nat. Commun. **4**, 2380 (2013).

[56] B. J. DeSalvo, K. Patel, G. Cai, and C. Chin, Observation of fermion-mediated interactions between bosonic atoms, Nature (London) **568**, 61 (2019).